Athermal Characteristics of TiO_2-Clad Silicon Waveguides at 1.3µm

S. Feng[1], K. Shang[1], J. T. Bovington[2], R. Wu[2], K-T. Cheng[2], J. E. Bowers[2] and S.J.B. Yoo[1,*],
[1]Department of Electrical & Computer Engineering, University of California, Davis, California, USA
[2]Department of Electrical & Computer Engineering, University of California, Santa Barbara, California, USA
*Corresponding author: sbyoo@ucdavis.edu

***Abstract*— We investigate athermal characteristics of silicon waveguides clad with TiO_2. The measured ring resonance wavelengths near 1.3 µm over 20-50°C exhibit second-order thermo-optical effects and spectral dependency, implying second-order effects from TiO_2 and Si combination.**

I. Introduction

Silicon photonic devices are sensitive to environmental temperature variations since silicon has a relatively large thermo-optical coefficient (TOC) of ~1.84×10^{-4}/°C. One method of thermal stabilization is to adopt an upper cladding made of a material with negative TOC to compensate for the positive TOC of silicon. Titanium dioxide has a strong negative TOC of ~-(1~2)$\times10^{-4}$/°C, and is compatible with CMOS processes offering superior reliability than polymers, thus it has been attracting strong interest. Previously, we demonstrated athermal silicon photonic devices with TiO_2 cladding in the 1550nm wavelength range [1, 2]. This paper investigates athermal silicon waveguides clad with TiO_2 and measure temperature-dependent resonant wavelength shifts less than 5 pm/°C exhibiting second order effects near 1310 nm.

II. Waveguide Geometry and Fabrication

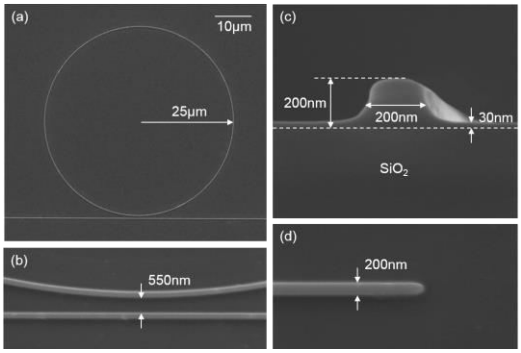

Fig. 1 Waveguide geometries. (a) Top-view SEM image of ring resonator before TiO_2 cladding deposition; (b) Ring-to-bus waveguide coupling region; (c) Cross-sectional SEM image of waveguide before TiO_2 cladding deposition; (d) Top-view SEM image of inverse taper.

The device fabrication utilized a 150mm silicon-on-insulator (SOI) wafer with 200nm thick top silicon and 3µm of buried oxide layers. A silicon nitride hard mask of 30nm is deposited and patterned with 248nm projection lithography followed by CF_4/CHF_3 reactive ion etching. The waveguide is reactive-ion-etched with HBr and then thermally oxidized with the hard mask still on top in order to smoothen the sidewall and reduce the waveguide width below the lithography limit of 250 nm dimension. The hard mask is then stripped in hot phosphoric acid. Figure 1 shows the SEM images of the fabricated device before TiO_2 cladding deposition. The ring resonator has a radius of 25 µm and a gap spacing of 550nm between ring and straight waveguides. The waveguide has a width of 200nm and a slab thickness of 30nm. The device has inverse tapers with a tip of 200nm at two output ends.

The waveguide formation is followed by a deep etch of the silicon facet and the TiO_2 sputtering of the 1.3 µm thick top cladding so that the optical mode experiences negligible interaction with the TiO_2-air boundary. Ref. 1 describes the TiO_2 sputtering conditions in detail.

III. Results and Discussion

Transmission spectra measurements utilize a tunable laser and a photodiode with a device in the interferometer of the optical vector network analyzer (OVNA). The light from the laser uses a single-mode lensed fiber to launch into the inverse taper coupler on the silicon photonic waveguide. The thermo-electric cooler (TEC) mounts the silicon photonic device to control the device temperature. The transmission spectra measurements utilize silicon photonic resonators prepared on the same wafer but having different overcladding layer materials: SiO_2 and TiO_2. Figure 2 shows the measured transmission spectra of the two devices. The device with SiO_2 cladding shows a significant resonant wavelength redshift of 1 nm over 15°C variations, while those with TiO_2 cladding shows less than 0.1 nm over the same range.

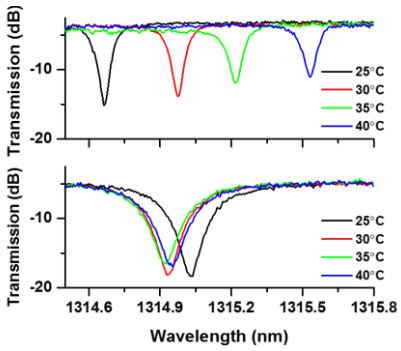

Fig. 2 Transmission spectra at various temperature of the devices with (a) SiO_2 and (b) TiO_2 upper cladding.

We compared three ring resonators overclad with TiO_2 with waveguide widths 200 nm, 220 nm and 240 nm. For each device, we measured the transmission spectra from 1270 nm to 1340 nm over the 20-50°C temperature range. We observe three phenomena of temperature-induced wavelength shift including (1) a quadratic wavelength shift with temperature driven by second-order material TOCs and by changes in the confinement factor, (2) spectral dependency attributable to a combination of waveguide and material dispersion, and (3) waveguide width dependency attributable to changes in the mode confinement. Figure 3

shows resonance wavelength as a function of temperature for the devices of 200nm width with SiO_2 and TiO_2 cladding. The ring with SiO_2 cladding shows a wavelength shift of 50 pm/°C. The ring with TiO_2 cladding shows quadratic curves.

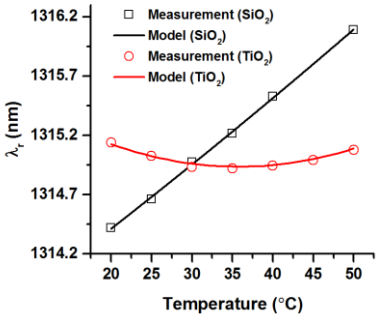

Fig. 3 Resonance wavelength as a function of temperaute for the devices of 200nm width with SiO_2 and TiO_2 cladding.

In order to explain the quadratic dependency of wavelength upon temperature, second-order material TOCs have to be taken into consideration. Material TOC can be expressed as:

$$dn / dT = \beta + \gamma \cdot T \tag{1}$$

The resonance wavelength of a ring resonator can be expressed as:

$$\lambda_r = n_{eff} \cdot 2\pi R / m \tag{2}$$

where m is the mode order. Hence its thermal dependency has the form:

$$d\lambda / dT = \lambda / n_g \cdot \left(dn_{eff} / dT + \alpha_{sub} \cdot n_{eff} \right) \tag{3}$$

where the α_{sub} is the thermal expansion coefficient of the silicon substrate which dominates the expansion of the path length. dn_{eff} / dT can be expressed as a linear superposition of TOCs of constituent materials:

$$dn_{eff} / dT = \sum_k \Gamma_k \cdot dn_k / dT = \sum_k \Gamma_k \cdot \left(\beta_k + \gamma_k \cdot T \right) \tag{4}$$

Here, Γ_k is the confinement factor of each constituent part. We assume that the second order effect due to $\partial\Gamma / \partial T$ is negligible. Plug Eq. (4) into Eq. (3) and we can get $d\lambda / dT$ as a first-order polynomial function of temperature T which can explain the quadratic relationship between wavelength and temperature. The TOC of silicon at 1.3μm is reported as $1.834 \times 10^{-4} + 4.887 \times 10^{-7} \cdot T$ [3], where T is in unit °C. The $\beta_{SiO_2} = 1 \times 10^{-5} \mathrm{K}^{-1}$ and γ_{SiO_2} is assumed to be 0. The TOC of TiO_2 is calculated to be $-3.07 \times 10^{-4} + 4.45 \times 10^{-6} \cdot T$ based on fitting the measurement data.

Our simulation indicates that the $\partial\Gamma / \partial T$ induced second-order coefficient $d^2\lambda / dT^2 = 4.3 \times 10^{-5}\ \mathrm{pm \cdot K^{-2}}$, which agrees with the result in [4]. This is much smaller than the one observed in our measurements (1.6×10^{-3} pm·K^{-2}), which verifies the approximation of neglecting $\partial\Gamma / \partial T$ in Eq. (4).

The temperature-dependent wavelength shift can be varied at different spectral ranges. Figure 4 shows the measurement of the device with a waveguide width of 200nm at various spectral ranges. At 1270nm wavelength, resonance redshifts when temperate increases. At 1310nm and 1340nm wavelengths, resonance wavelength first blueshifts and then redshifts as temperature rises. For a fixed waveguide geometry, when the wavelength becomes longer, mode confinement increases in TiO_2 cladding, which contributes to the resonance blueshift and athermalization.

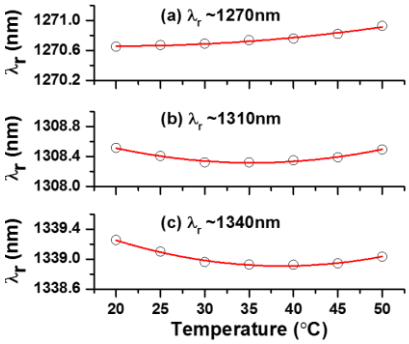

Fig. 4 Measured (black circle) and quadratically fitted (red line) resonance wavelength shift as a function of temperaute. The device with a waveguide width of 200nm is measured at various spectral ranges around (a) 1270nm, (b) 1310nm and (c) 1340nm.

The temperature-dependent wavelength shift is also varied for different waveguide widths. Figure 5 shows the measurement of three devices with waveguide widths of 200nm, 220nm, and 240nm at a spectral range around 1310nm. For a fixed spectral range, when waveguide width becomes narrower, mode confinement increases in TiO_2 cladding, which contributes to the resonance blueshift and athermalization.

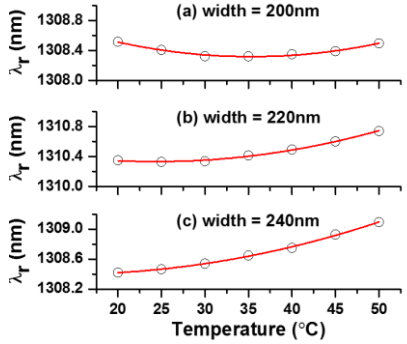

Fig. 5 Measured (black circle) and quadratically fitted (red line) resonance wavelength shift as a function of temperaute. Three devices with different waveguide widths (a) 200nm, (b) 220nm and (c) 240nm are measured at a spectral range around 1310nm.

IV. CONCLUSTIONS

In order to athermalize silicon photonic devices over a wide temperature range, the waveguide widths, TOC values of the materials, and operating wavelengths have to be carefully considered. In particular, second order effects of TOC of TiO_2 need to be included in design and operation near the athermal condition.

V. REFERENCES

[1] S. S. Djordjevic et al., Opt. Express 21, 13958–13968 (2013).
[2] J. Bovington et al., Opt. Express 22, 661-666 (2014).
[3] B. J. Frey et al., Proc. SPIE 6273, 62732J (2006).
[4] V. Raghunathan et al., Opt. Express 18, 17631-17639 (2010).

This work was supported in part by Intel University Research Office.